American Journal of Pathology, Vol. 127, No. 2, May 1987
Copyright © American Association of Pathologists

Ultrastructural Evidence That the Granules of Human Natural Killer Cell Clones Store Membrane in a Nonbilayer Phase

JOHN P. CAULFIELD, ANN HEIN, REINHOLD E. SCHMIDT, and JEROME RITZ

From the Departments of Pathology and Medicine, Harvard Medical School, the Department of Rheumatology and Immunology, Brigham and Women's Hospital, and the Division of Tumor Immunology, Dana Farber Cancer Institute, Boston, Massachusetts

Electron-microscopic examination of five LGL clones, JT3, JT_B18, CNK6, CNK7, and CNK10, expressing natural killer activity and T11 and NKH1 phenotype, showed that three of the clones, JT3, CNK6, and CNK7, had crystalline structures in their densest granules. These structures generally consisted of hexagonally packed lattices with a 6.9-nm point-to-point spacing. JT_B18 and CNK10 had no structures in their granules. The attack of one clone, JT3, on two resistant target tumor cell lines, KG1 and Laz509, was also examined under three conditions. First, JT3 cells and targets were incubated together. There was little adherence, degranulation, or killing. Second, cells were incubated with anti-$T11_2$ and $T11_3$, antibodies against the E-rosette receptor/antigen complex, which activate resting T cells and enhance cytolytic activity of NK clones and CTL. JT3 cells adhered to the targets, formed zones of apposition between NK and target cell membranes, polarized, and degranulated into the space between the two cells, killing the targets. Third, cells were incubated with both anti-$T11_{2/3}$ and anti-LFA-1, an antibody that inhibits adherence. The JT3 cells did not form zones of apposition with the targets, but degranulated in discrete areas on their own surface. In all cases, discharged crystalline granules transformed to sheets of membrane and vesicles. These studies suggest that phospholipids are packed in hexagonal lattices in the granules of the resting cells and transform to bilayer structures during exocytosis. The crystalline nature of the granule may immobilize lytic molecules and protect the resting cell from lysis. Further, the vesicles may serve to transport the lytic molecules from the effector to the target cell. Anti-LFA-1 does not inhibit target recognition or exocytosis, but instead blocks membrane interactions of the effector cell with its target. (Am J Pathol 1987, 127:305–316)

IN VARIOUS MODEL SYSTEMS natural killer (NK) cells have been shown to be important effector cells in the lysis of malignant or virally transformed cells.[1] In normal individuals NK cells comprise approximately 10–12% of peripheral blood mononuclear cells and appear morphologically as large granular lymphocytes (LGLs). Although there is considerable phenotypic and functional heterogeneity within the NK cell population, the general mechanism by which these cells and other cytolytic lymphocytes kill their targets is thought to be similar and can be summarized as follows. LGLs bind to the targets and reorient their cytoplasm so that their granules, Golgi apparatus, and centrioles are closest to the target.[1-3] The granules in the effector cell are then exocytosed against the surface of the target cell,[1-5] thereby releasing lytic molecules that insert into the target membrane, polymerize, and form large pores that lyse the target.[5-9]

Although lytic molecules, which are called per-

Supported in part by NIH Grants AI23083, AM3638, and CA41619. R.E.S. is a recipient of a fellowship (Schm 596/1-1) from the Deutsche Forschungsgemeinschaft. His present address is Abteilung Immunologie und Transfusionsmedizin, Zentrum Innere Medizin and Dermatologie, Medizinische Hochschule Hanover, Postfach 610180, D-3000, Hannover, West Germany. J.R. is a Scholar of the Leukemia Society of America.

Accepted for publication December 16, 1986.

Address reprint requests to John P. Caulfield, MD, Seeley G. Mudd Bldg., Rm. 517, 250 Longwood Ave., Boston, MA 02115.

forins,[8,9] cytolysins,[3] or C9-related protein,[10] are contained within effector cell granules, it is not clear how these proteins are transported to the target cell membrane after exocytosis. However, it has been postulated that these molecules are transported by membranes, because vesicles seen between the LGLs and targets have pores in their membranes that correspond to the size of the pores made by lytic molecules in target membranes.[5,7] The genesis of these vesicles is unclear, but they may be derived from the granules themselves[5,7] or from the Golgi apparatus.[5] It is also not clear how the LGLs protect themselves from lysis by their own lytic molecules. The lytic molecules could be maintained in the granule in a monomeric state by complexing with other molecules, such as highly charged proteoglycans.[11] Alternatively, the granule matrix could exist in a crystalline or gel state which would immobilize its constituents and prevent polymerization of lytic molecules.

Here, we have examined five human LGL clones that possess NK activity. Three of the clones have granules that contain crystalline lattices generally packed in a hexagonal array. When lysis of resistant target cells is induced with monoclonal antibodies against the T11/E-rosette receptor/antigen complex,[12] the granules are exocytosed and the lattices transform into membranes. These results suggest that the clone granules store membrane phospholipids as hexagonal lattices that undergo phase transformation to bilayers during secretion. In the resting cell the lattices may immobilize lytic molecules and prevent autolysis of the LGL. After activation, the bilayers may transport the lytic molecules to the target cell. Finally, the presence of anti-LFA-1 monoclonal antibodies in cytolytic reactions prevents the close opposition of NK and target cell plasma membranes, thereby reducing conjugate formation and target lysis.

Materials and Methods

Preparation of Lymphocyte Conditioned Medium (LCM)

LCM was produced by stimulating whole peripheral blood mononuclear cells (PBMCs) at a concentration of 2×10^6/ml for 3 hours with phytohemagglutinin (5 μg PHA/ml) (Wellcome Research Laboratories, Tuckahoe, NY) and phorbol myristate acetate (5 ng/ml) (Sigma Chemical Co., St. Louis, Mo). The cells were then washed four times for removal of the mitogens and resuspended in RPMI 1640 medium supplemented with 2.5% human AB serum. After 40 hours of additional incubation at 37 C, the supernatants were harvested, passed through 0.45-μ filters, and stored at −70 C.

Generation of Human Cloned Cell Lines

Methods for generation of human cloned NK cell lines have been described in detail.[13] Briefly, clones were obtained with the use of a limiting dilution technique by plating 1 cell/well on a feeder layer of autologous irradiated (5000 cGy) PBMCs plus irradiated Epstein Barr virus (EBV)-transformed B cells. Colonies were screened for cytotoxicity against K562 target cells and were expanded by the addition of culture medium containing LCM (10–15% final dilution) every 3 days. All clones that showed NK activity against K562 targets were $NKH1^+$ whether they were cloned from PBMCs, purified LGLs, or $NKH1^+$ sorted cells. The culture medium was RPMI 1640 medium supplemented with penicillin-streptomycin, L-glutamine, sodium pyruvate, and 20% human AB serum. All cell lines that were used in these studies have been subcloned at least four times at 100 cells/well on a feeder layer of allogenic, irradiated PBMCs plus irradiated EBV-transformed B cells. JT3, CNK6, CNK7, and JT_B18 clones have been described in detail.[13] CNK10 is an additional $T3^-$ NK clone from a different individual. The phenotypes of all NK clones are summarized in Table 1.

Cell Lines

Several continuously growing cell lines were used as targets for NK effector cells. K562 and KG1 were established from patients with myelogenous leukemias. Laz509 is an EBV-transformed B-cell line.

Monoclonal Antibodies

The monoclonal antibodies utilized in these studies have been previously described in detail. Anti-$NKH1_A$ is an IgM monoclonal pan NK cell antibody with specificity identical to that of anti-NKH1 (N901).[13] Anti-NKH2 characterizes a subset of LGLs. Anti-$T11_1$ defines an epitope related to the sheep erythrocyte (E rosette) binding site that is present on all T cells and on over 80% of NK cells. Anti-$T11_2$ identifies an epitope not directly related to the SRBC binding site, but has an identical tissue distribution. Anti-$T11_3$ defines a T11 epitope that is not found on

Table 1—Phenotype of NK Clones

Clone	T3	T8	T11	NKH1	NKH2	B73.1
JT3	−	−	+	+	−	−
CNK6	−	−	+	+	+	−
CNK7	−	−	+	+	+	−
JT_B18	−	−	+	+	+	−
CNK10	−	−	+	+	+	+

resting T cells, but is expressed rapidly after cell activation or in response to anti-T11$_2$. Monoclonal antibody 2F12 is specific for the alpha chain of the LFA-1 molecule. The T-cell antibodies anti-T8 and anti-T3 have been characterized previously in detail.[15]

Cytotoxicity Assays

All experiments were performed in triplicate using V-bottom microtiter plates. Medium for cytotoxicity assays was RPMI 1640 plus 5% pooled human Ab serum and penicillin-streptomycin. Assays were performed at various effector to target (E/T) cell ratios with 5000 ^{51}Cr-labeled target cells per well. Cytotoxicity was measured following 4 hours of incubation at 37 C. Specific cytotoxicity was calculated according to a standard method.[15]

Electron Microscopy

The following samples were examined: 5 NK cell clones, JT3, CNK6, CNK7, CNK10, and JT$_B$18, as well as JT3 cells incubated at 37 C for 40 minutes with either KG1 or Laz509 target cells, with or without anti-T11$_{2/3}$ or with anti-T11$_{2/3}$ and anti-LFA-1 at an NK/target ratio of 10 : 1. For each sample, at least 10^6 NK cells were fixed by the addition of an equal volume of mixed aldehydes[16] at 4 C, then kept on ice for 40 minutes. The cells were centrifuged in 400-μl tubes in a Beckman microfuge, and the pellets were removed from the tubes, processed routinely in buffered osmium tetroxide, uranyl acetate, graded ethanols, and propylene oxide, and embedded. Silver to silver-gold thin sections were cut on diamond knives, picked up on naked grids, either stained with uranyl acetate and lead citrate or left unstained, and examined in a JEOL 100C electron microscope equipped with a eucentric goniometer.

Results

Morphology of NK Cell Clones

All five NK cell clones had a similar appearance at low magnification and resembled published descriptions of peripheral blood LGLs, CTLs, and NK cells. In brief, the cells contained a single eccentric nucleus surrounded by a polyribosome-rich cytoplasm (Figure 1). The Golgi apparatus, mitochondria, centrioles, and granules were generally clustered in one region of the cell (Figure 2). All clones contained a few lipid droplets per cell profile. The granules differed in size and frequency from clone to clone. JT$_B$18 had up to 18 granules per cell profile with an average of 8 granules per profile. JT3 had about 5 granules per cell profile, whereas CNK6, CNK7, and CNK10 had 2 granules per cell profile. However, in all five clones some cell profiles had no granules. The granules were largest in JT3 and JT$_B$18 cells and ranged from 0.05 to 0.1 μm in diameter. In CNK6, CNK7, and CNK10 cells the granules were 0.05 μ.

At high magnification most of the granules in all of the clones were composed of homogeneous electron-dense material surrounded by a perigranular membrane as previously described for JT$_B$18 cells.[11] In addition, the electron density varied between granules from black to approximately that of the cytoplasm. Parallel tubular arrays (PTAs), which consist of closely packed electron-dense pipelike structures,[17,18] were not observed in any of the clones. However, in three clones, JT3, CNK6, and CNK7, some of the densest granules contained crystalline lattices or gratings (Figure 3). In stained sections crystalline structures were seen in about 10% of the densest granules, but in unstained sections all of the densest granules contained these structures. The lattices were composed of hexagonally packed points, each point equidistant from six other points (Figure 3a and b). The gratings consisted of a set of parallel lines (Figure 3b–d), usually straight (Figure 3c), but occasionally in a whorled fingerprint pattern (Figure 3b and d). The grating pattern also appeared superimposed on the lattice pattern with the sets of parallel lines running in three directions that were at 120 degrees with respect to one another. When sections were tilted with a eucentric goniometer, some gratings became lattices and some lattices became gratings, suggesting that both gratings and lattices were simply different views of the same structure. The lattice spacing averaged 6.9 $\pm$ 0.3 nm (n = 8) and was the same dimension in all three clones. The thickness of the electron-dense lines or points was more variable and ranged from 2.5 to 3.6 nm. In addition to hexagonally packed lattices, cubic lattices were seen occasionally (Figure 3e). In some cases, granules containing lattices were juxtaposed to less electron-dense granules (Figure 3b). Granules with low electron density did not have crystalline structure. Finally, some granules contained strands of membrane, usually on the periphery beneath the perigranular membrane (Figure 3f).

Morphology of JT3 NK Cells Attacking Laz509 and KG1 Target Cells

We examined one of the clones with crystalline granules in a cytolytic reaction to see what structural changes occurred in the granule contents during activation. Because the granules of JT3 cells were larger

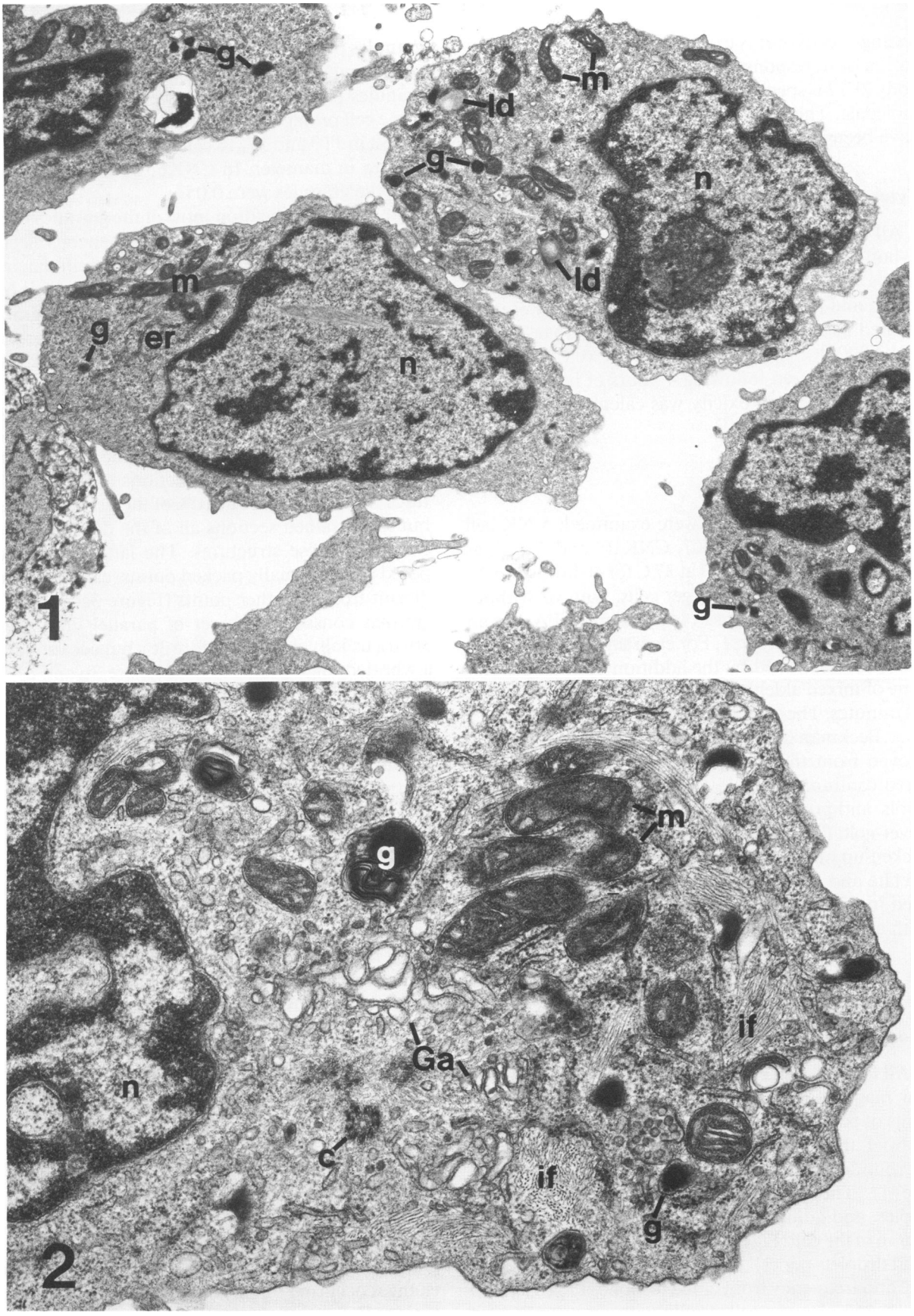

Figure 1—Human NK cloned cells, JT3 line. The nuclei (*n*) are eccentric and the granules (*g*), lipid droplets (*ld*), mitochondria (*m*), and rough endoplasmic reticulum (*er*) are localized to one end of the cell. Note the variable number of granules per cell profile. (Section stained on grid with uranyl acetate and lead citrate, ×8000) **Figure 2**—Region of a JT3 cell in which the granules (*g*), mitochrondria (*m*), Golgi apparatus (*Ga*), centriole (*c*), and intermediate filaments (*if*) are found, *n*, nucleus. (Section stained on grid with uranyl acetate and lead citrate, ×23,500)

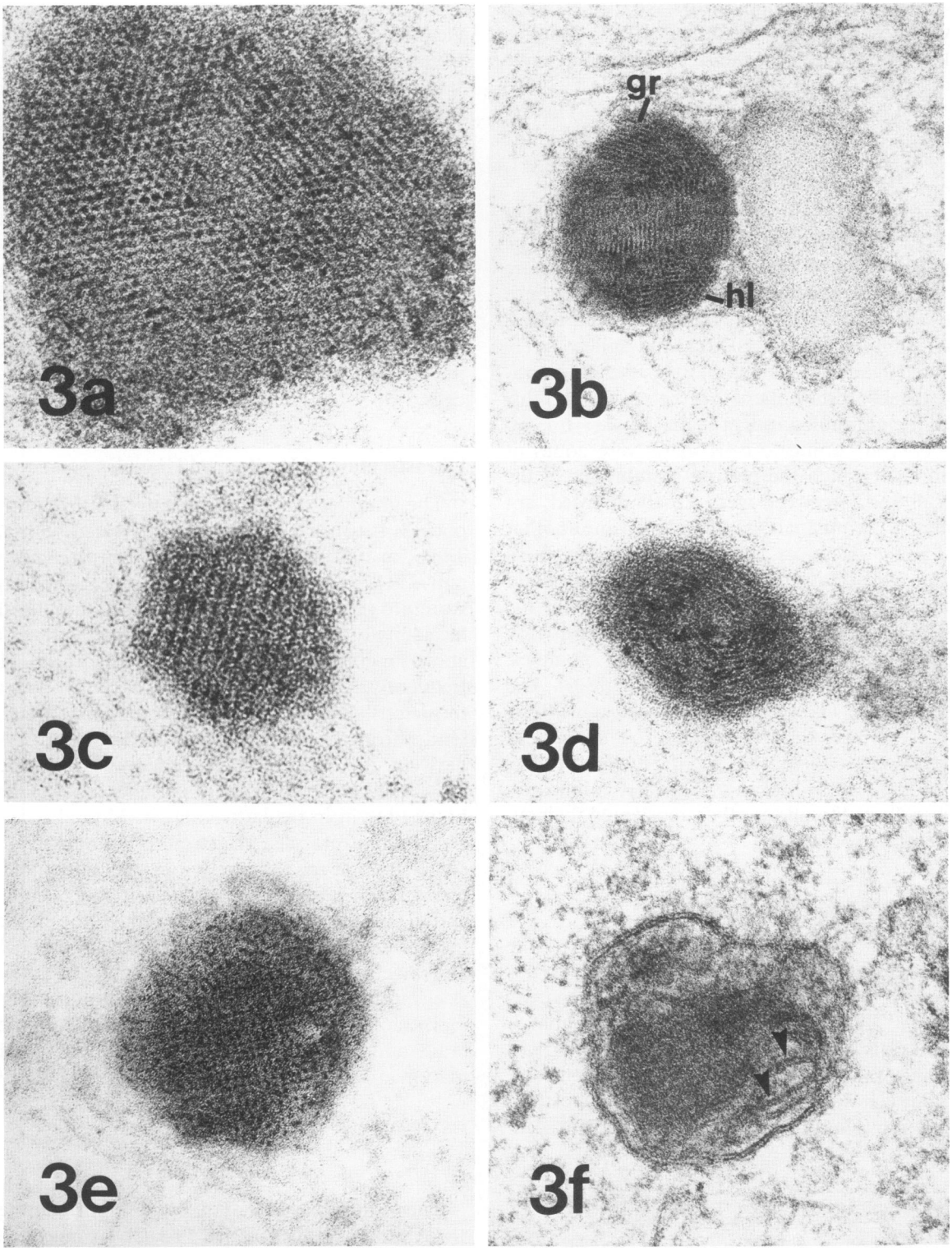

Figure 3—Resting granule ultrastructure in three NK cell clones. JT3, **a**,**b**,**e**, and **f**; CNK6, **c**; and CNK7, **d**. Note the hexagonally packed lattice (*hl*) in **a** and **b**. The period of the lattice is 6.9 ± 0.3 nm. Each point has six nearest neighbors. A linear grating (*gr*) pattern is seen in **b**, **c**, and **d** and forms a whorled "fingerprint" pattern in **b** and **d**. In **e**, the points in the lattice are cubically arrayed. In **b**, an electron-lucent granule with no crystalline substructure is juxtaposed to an electron-dense crystalline granule. In **f**, there are membranes (*arrowheads*) on the periphery of the granule matrix within the perigranular membrane. (**a–d** and **f**, sections stained on grid with uranyl acetate and lead citrate; **e**; section unstained; **a**, ×238,000; **b**, ×139,000; **c**, ×242,000; **d**, ×147,000; **e**, ×228,000; **f**, ×118,000)

and more numerous than those of CNK6 and CNK7, JT3 was chosen for further studies on target killing. Attacks were promoted against two resistant target cell lines, KG1 and Laz509, by activation of JT3 cells with anti-T11$_{2/3}$ as previously described.[12] This resulted in an increase in target killing from 10% in the absence of anti-T11$_{2/3}$ to 27% in its presence for KG1, and from 6% to 43% for Laz509 (Table 2).

Ultrastructural examination of JT3 cells incubated with target cells showed that effector cells could be distinguished from targets, because the targets were larger and contained fewer organelles. In the absence of anti-T11$_{2/3}$, few JT3 cells adhered to the targets after 40 minutes. Those cells that did adhere rarely exocytosed against the target. In the presence of anti-T11$_{2/3}$, the JT3 cells adhered to the targets and discharged their granules against them (Figure 4). Typically, between conjugate cells there were zones of apposition in which the plasma membranes of the clone cell and target cell were closely apposed, approximately 20 nm apart, and parallel to one another over 0.5–1-μ distances (Figure 5). Between these zones, the two plasma membranes were separated and formed pockets (Figure 4). These pockets were the sites at which the JT3 cells exocytosed against the targets and often contained discharged granules, membrane fragments, and vesicles (Figure 6). The cytoplasm of the JT3 cells was oriented against these pockets, with the Golgi apparatus, centriole, and granules closest to the pocket and the nucleus further away. In addition to forming NK/target conjugates, NK cells adhered to one another, reoriented their cytoplasm, and exocytosed.

Effect of Anti-LFA-1 on JT3 NK Cells Attacking Targets

The presence of 2F12, anti-LFA-1, caused an approximately 50% decrease in anti-T11$_{2/3}$ induced target killing (Table 2).[11] When examined morphologically, JT3 cells incubated with anti-T11$_{2/3}$ and 2F12 did not generally adhere to target cells. When NK/target conjugates were seen, the zones of apposition described above and shown in Figure 5 were not seen.

Table 2—Cytotoxicity of NK Clone JT3*

Target	Medium	Anti-T11$_{2/3}$	Anti-T11$_{2/3}$+anti-LFA-1
K562	82†	NT	NT
KG1	10	27	15
Laz509	6	43	18

*Cytotoxicity assays were performed at an E/T ratio of 5:1.
†Percent specific cytotoxicity.
NT, not tested.

However, cells associated loosely and vesicles and electron-dense material were present in the space between JT3 and target cells (Figure 7). Many JT3 cells had a single region on their surface to which exocytosed granule contents and membrane vesicles were adherent (Figure 8). Further, discharged granules were found more frequently on the surface of unconjugated JT3 cells than in pockets. In two experiments, 83% (26 of 31) and 100% (19 of 19) of the recognizable extracellular granules were found on the surface of unconjugated JT3 cells after treatment with anti-T11$_{2/3}$ and anti-LFA-1. In comparison, after treatment with anti-T11$_{2/3}$ alone, 50% (7 of 14) and 69% (18 of 26) of extracellular granules were found in pockets between JT3 cells and target or other NK cells.

Ultrastructure of Discharged Granules

The granules that were discharged either into the pockets between JT3 and targets treated with anti-T11$_{2/3}$ or onto the surface of JT3 cells treated with anti-T11$_{2/3}$ and anti-LFA-1 transformed their granule structure (Figure 9). Some discharged granules had hexagonally packed crystalline lattices as described above for granules in the resting cell (Figure 9a). More frequently, the gratings or lattices unraveled and formed trilaminar strands of unit membrane that extended from the core of the granule (Figure 9b). Alternatively, the entire granule lattice was swollen and loosened (Figure 9c), with trilaminar strands of membrane present in the lattice matrix. Matted sheets of membrane were seen that were often denser at the center than at the periphery, but they contained no recognizable lattice structure at their core (Figure 9d and e). Vesicles were often adjacent to the sheets of membrane (Figure 9e). Many pockets between JT3 and target cells were filled with similar vesicles as well as electron-dense material from the granules (Figure 6). Intracellular granules often contained both membrane and vesicles, suggesting that granule transformation might also occur before exocytosis (Figure 9f).

Discussion

These studies show that the cytoplasmic granules of three human NK cell clones, JT3, CNK6, and CNK7, contain crystalline lattices that are generally hexagonally packed. During attack promoted with anti-T11$_{2/3}$ against two resistant targets, the granules are exocytosed and the lattice unfolds and transforms into membranes. Anti-LFA-1 inhibits adherence of the clone to its target and the formation of zones of oppo-

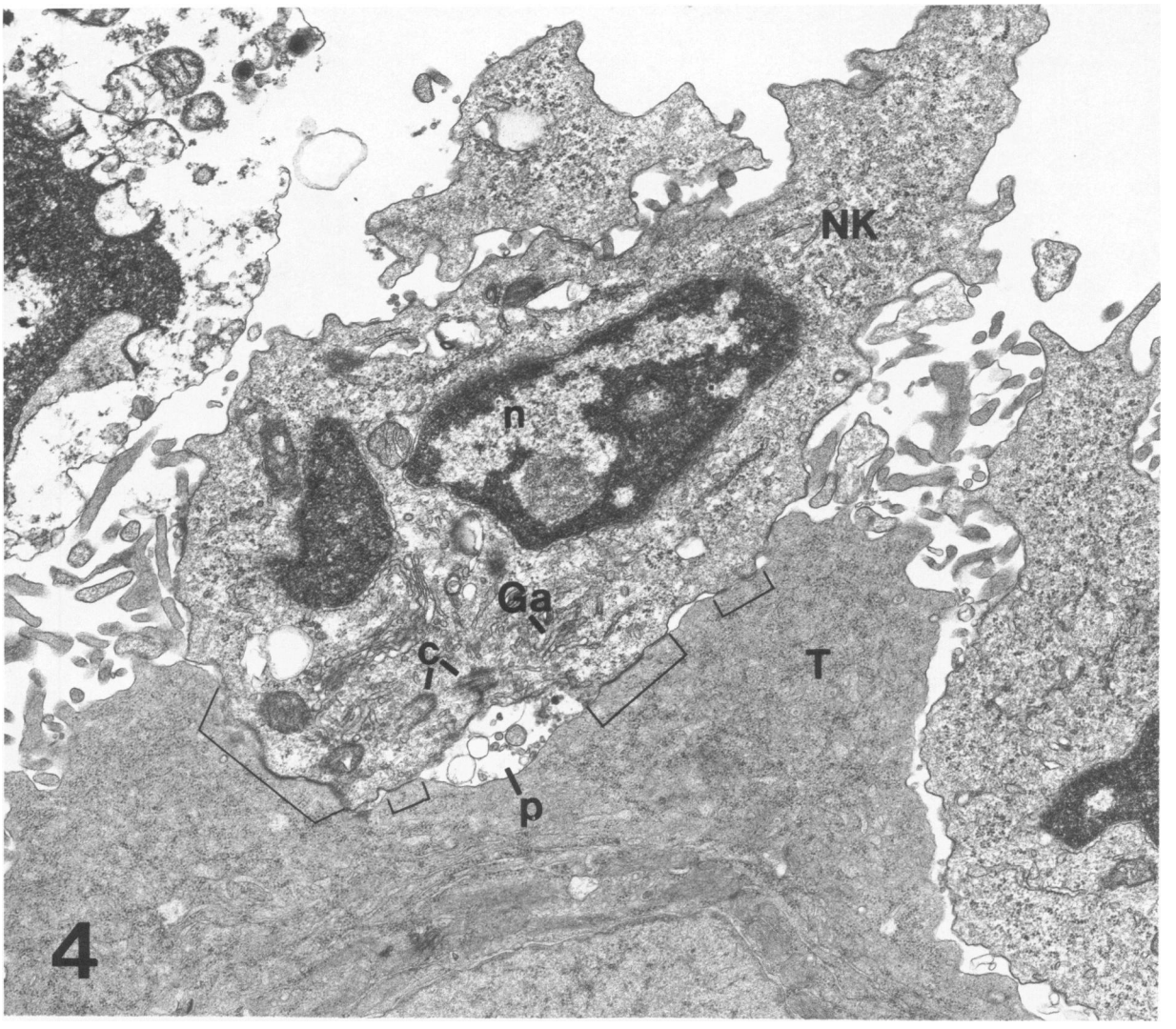

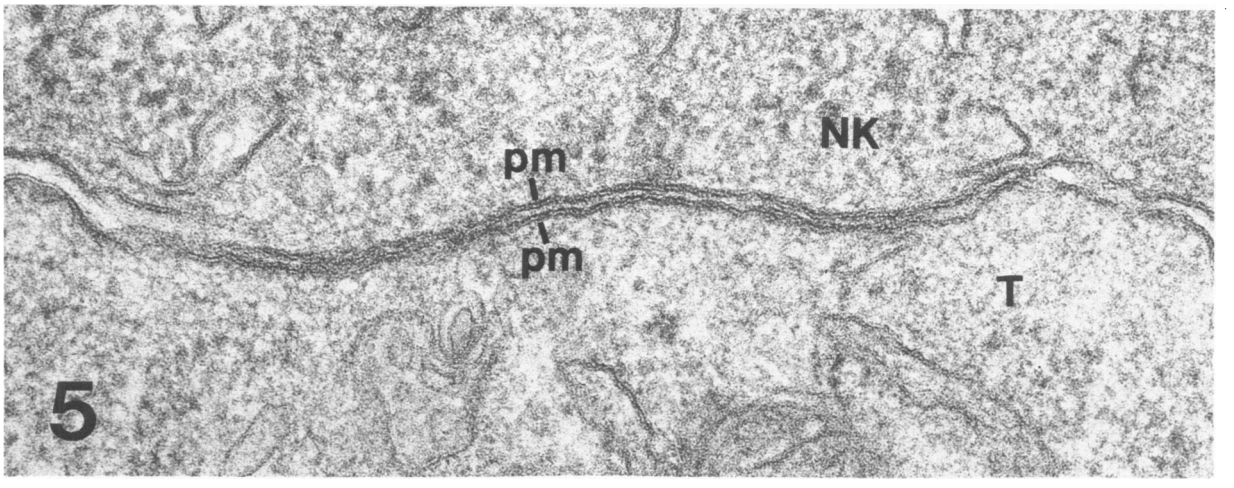

Figure 4—JT3 cell (*NK*) adhering to an Laz509 target cell (*T*) after 40 minutes' incubation with anti-$T11_{2/3}$. Note the zones of close apposition of the plasma membranes (*brackets*) Between these zones the plasma membranes of the two cells are separated to form a pocket (*p*). The pocket contains membrane and electron-dense material. The NK cell is oriented so that the Golgi apparatus (*Ga*) and centrioles (*c*) are closest to the pocket and the nucleus (*n*) further away. (Section stained on grid with uranyl acetate and lead citrate, ×14,500) **Figure 5**—High magnification of a zone of apposition of a JT3 cell (*NK*) and Laz509 target cell (*T*) after 40 minutes' incubation with anti-$T11_{2/3}$. The plasma membranes (*pm*) of the two cells are less than 20 nm apart. (Section stained on grid with uranyl acetate and lead citrate, ×96,000)

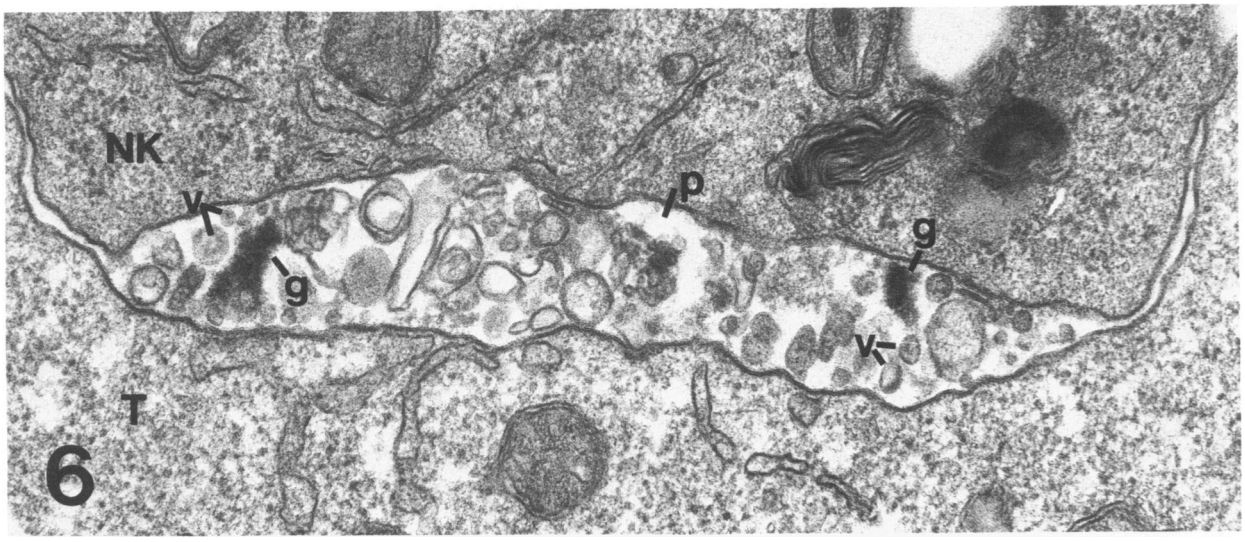

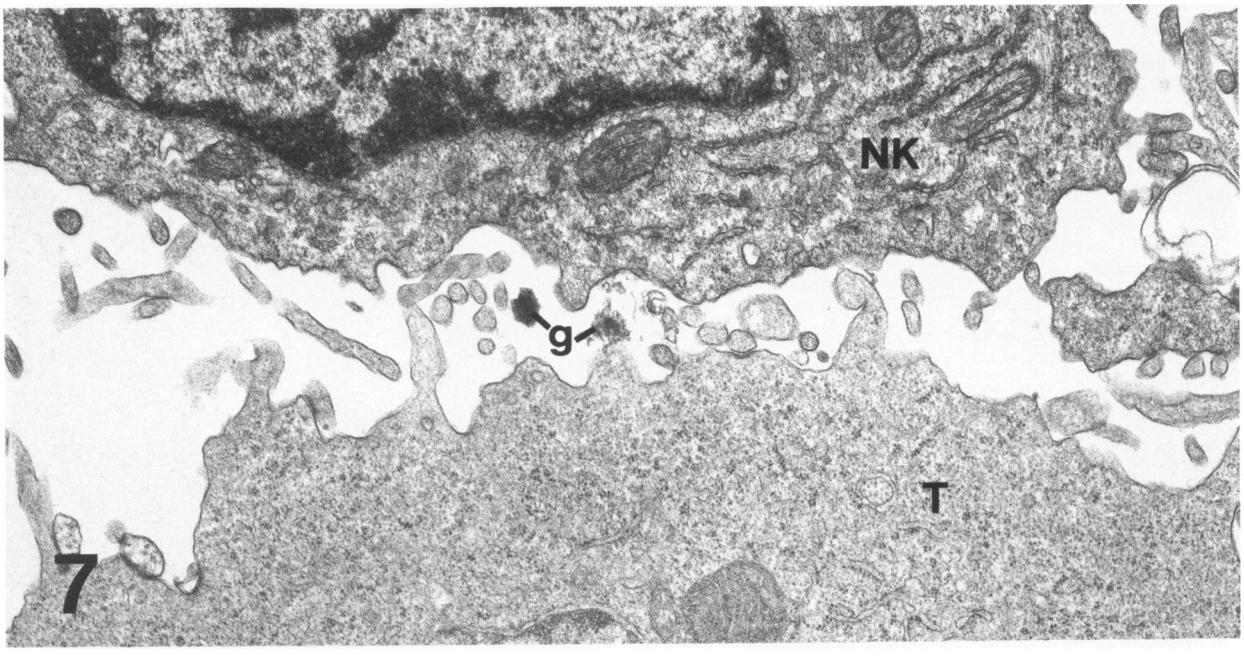

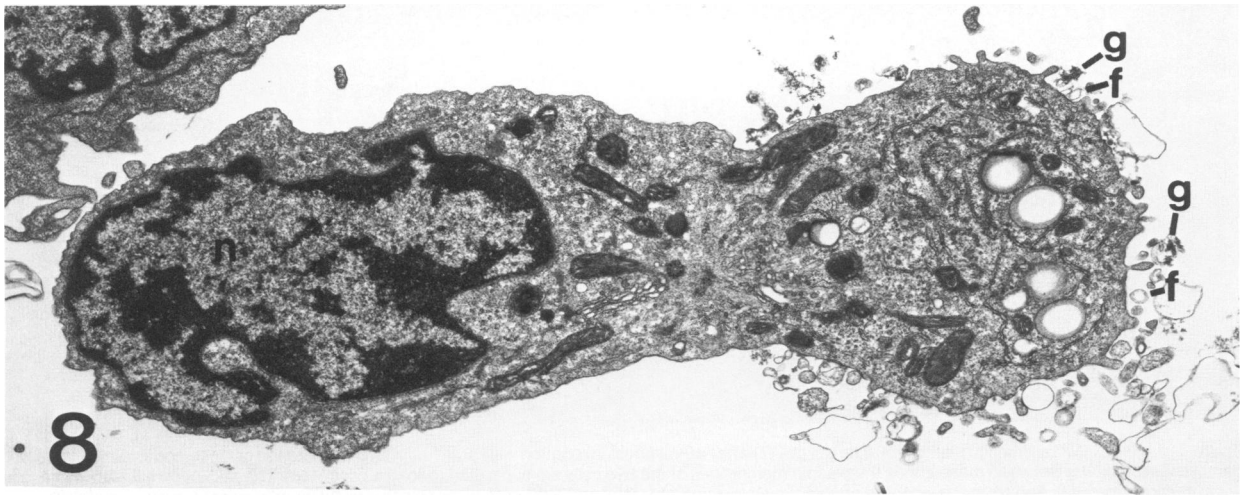

Figure 6—JT3 cell (*NK*) adhering to an Laz509 target cell (*T*) after 40 minutes' incubation with anti-$T11_{2/3}$. The pocket (*p*) between the two cells contains the remnants of exocytosed granule material (*g*) and membrane fragments and vesicles (*v*). (Section stained on grid with uranyl acetate and lead citrate, ×45,000) **Figure 7**—JT3 cell (*NK*) after 40 minutes' incubation with Laz509 target cells (*T*), anti-$T11_{2/3}$, and anti-LFA-1. The cells are loosely attached to one another, and zones of apposition (see Figure 5) are not seen. Discharged granules (*g*) are present. (Section stained on grid with uranyl acetate and lead citrate, ×19,000) **Figure 8**—JT3 cell after 40 minutes' incubation with KG1 target cells, anti-$T11_{2/3}$, and anti-LFA-1. Note the granule remnants (*g*) and fragments of membrane (*f*) on the region of the cell surface adjacent to many subcellular organelles. The plasma membrane over the nucleus (*n*) does not have discharge material. (Section stained on grid with uranyl acetate and lead citrate, ×9000)

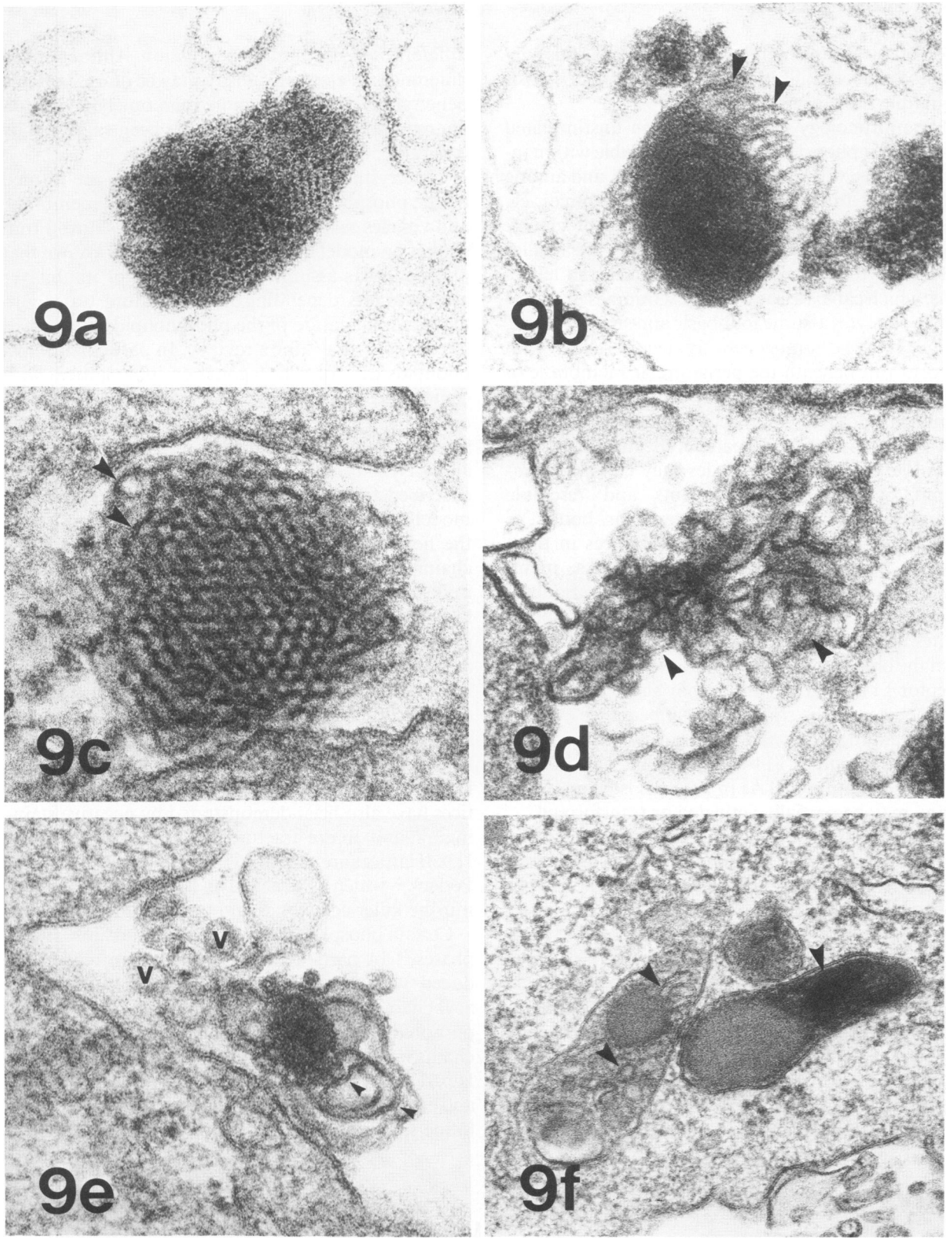

Figure 9—Exocytosed granules from JT3 cells after 40 minutes' incubation with KG1 (**a**—**d**) or Laz509 (**e**) targets with either anti-$T11_{2/3}$ (**a**,**c**, and **e**) or anti-$T11_{2/3}$ and anti-LFA-1 (**b**, and **d**). In **a** and **b** the hexagonally packed lattice and the grating pattern can still be seen, but in **b** there are trilaminar strands of membrane (*arrowheads*) extending from the edges of the granule. In **c** the granule lattice appears swollen and the packing is looser than in **a** and **b**. Membranes (*arrowheads*) are present in the granule. In **d** and **e** there are mats of membrane (*arrowheads*) extending from central electron densities. In **e** vesicles (**v**) are adjacent to the sheets of membrane. In **f**, intracytoplasmic granules from JT3 cells incubated with Laz509 targets and anti-$T11_{2/3}$ and anti-LFA-1 contain vesicles and membrane (*arrowheads*), suggesting partial transformation. (Sections stained on grid with uranyl acetate and lead citrate; **a** ×150,000; **b**, ×133,000; **c**, ×172,000; **d**, ×118,000; **e**, ×118,000; **f**, ×72,000)

sition of the plasma membranes. Anti-LFA-1 also decreases target cell killing but does not block exocytosis or granule transformation.

The morphology of the granules in unstimulated granular lymphocytes is extremely variable within individual cells, within populations of cells, and among cells derived from different species and sources, eg, blood[4,11,17-21] leukemias,[22,23] cell lines,[5,6] or clones. The granules in cells isolated from blood are smaller (0.1–0.2 μ) than granules in cloned lines and leukemias, which can be as large as 1 μ.[5] Granules in granular lymphocytes assume four basic appearances. First, granules may be homogeneously electron-dense, with a lucent rim beneath the perigranular membrane of the granule but with variation in density from one granule to another.[4,11,19,20] Second, granules may contain PTAs consisting of parallel electron-dense tubules.[17,18,21] Third, the granules may contain membranes or membrane fragments and resemble secondary lysosomes or multivesicular bodies.[5,22] Fourth, we have shown crystalline lattices in these granules (Figure 3). Granules with PTAs, membranes, or lattices may be in fact structural variants of a single granule type. In particular, PTAs and membranes are often found in granules of cells isolated from the blood by E-rosetting. However, the E-rosette receptor T11 antigen complex may also activate these lymphocytes.[12] The similarity in appearance of granules containing PTAs and membrane in isolated cells to granules found in T11-activated cells suggests that granules containing PTAs in the cells isolated by rosetting may be partially activated or transformed.

In their resting or unactivated state, the cytolytic granules are small and condensed and, in some cases, crystalline. The failure to observe crystalline lattices more often in lymphocytes may be due to masking by heavy metals because the lattices are seen more readily in unstained than in stained sections. Further, because osmium and uranium en bloc most probably provide the contrast necessary for seeing the lattices, manipulation of the exposure to these reagents may increase the demonstration of lattices in the granules of other cytotoxic lymphocytes. On the other hand, the differences in staining intensity among granules without any substructure may indicate biochemical differences in the granule population. Although such differences in electron density may be due to variable penetration of osmium, more than one type of granule may exist in these cells, as has been suggested by others.[20,22]

The crystalline lattices most probably are formed by the phospholipids that give rise to the membrane and vesicles seen after the granules transform. From studies on model lipid–water systems it is known that phospholipids assume either lamellar or nonbilayer arrangements, depending on temperature, water content, and the nature of the phospholipids themselves (see Gruner et al[24] for a review). In particular, phospholipids can form hexagonal or cubic lattices with center-to-center spacings of 4.5–7.0 nm, depending on the head group and acyl chains involved.[24-26] The spacing of the hexagonal lattices in the JT3, CNK6, and CNK7 cells is 6.9 nm and is within the range described for model phospholipid lattices. In these model lattices, the phospholipids form long rods with the head groups and water in the center and acyl chains radiating outward.[24] The rods are then ordered in hexagonal or cubic arrays (Figure 10). Hexagonal lattices of this type are called Hex II phases.[24]Hex I phases have rods with the head groups on the outside and centrally placed acyl chains. These two types of hexagonal lattices can be distinguished in thin sections because the head groups stain with osmium and the acyl chains do not. A Hex II lattice is seen as a hexagonal array of electron-dense points, and a Hex I lattice as an electron-dense honeycomb.[27] Hex II lattices have also been demonstrated by negative staining[26,28] and freeze fracture.[29] The negative stained Hex II lattices are similar to Figure 4D in Dennert and Podack,[5] which is a negative stain of a mixture of murine killer cell clones and target cell membranes.

Certain phospholipids preferentially assume Hex II phases.[24] In particular, these phases are readily induced with phospholipids containing unsaturated acyl chains and small, deionized head groups. Thus, phosphatidylethanolamine with unsaturated acyl chains would be the most likely phospholipid to form Hex II lattices.[24,26] However, the granules are complex and contain lytic molecules which appear to be membrane-spanning proteins,[8,9] proteoglycans,[11] and ly-

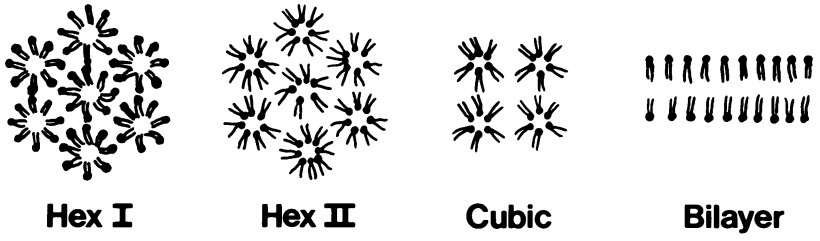

Figure 10—Diagramatic representation of phospholipids in various nonbilayer and bilayer phases. Dots represent the head groups and paired lines the acyl chains. The two lattices on the left are hexagonal. The Hex I lattice has central acyl chains and head groups on the outside of each subunit whereas the Hex II lattice has central head groups. The phospholipids in the cubic lattice are arranged like those in the Hex II lattice.

sosomal enzymes,[3,20] in addition to membranes. The proteins and proteoglycans may permit more complex mixtures of phospholipids in the granules than are possible in model systems. More importantly, the lytic molecules are most likely immobilized in the crystalline lattice and unable to polymerize and attack the NK cell itself.

Stimulation of the NK cell by anti-$TII_{2/3}$ and exposure to a target results in a transformation of the granule, possible fusion between granules, and exocytosis of both transformed and untransformed granule contents against the target cell. As noted above, granules can transform within the cell before secretion.[7] This phenomenon is not unusual and occurs in other cells, eg, human and rat mast cells.[30,31] However, not all NK granules are transformed before discharge, because crystalline granules without perigranular membranes are seen outside the cell. Once released, these granules also transform to membrane (Figure 9). Transformation can be explained as a phase transition of the phospholipids from a Hex II lattice to a lamellar arrangement (Figures 9 and 10). The phase transition could be promoted simply by the addition of water to the granule, by fusion with another more aqueous granule, by alterations in ion transport, or by exocytosis. The newly formed bilayer vesiculates after exocytosis and apparently transports lytic molecules to the target cell.[5-7] Vesiculation may be favored by the formation of pockets between the lymphocyte and its target. The pockets may permit the development of pH or ionic conditions differing from the surrounding medium which enhance delivery of membrane vesicles to the target plasma membrane.

The experiments with anti-LFA-1 and anti-$T11_{2/3}$ show that anti-LFA-1 does not block secretion, because transforming granules are found on discrete areas of the NK plasma membrane. Anti-LFA-1 inhibits the adherence of NK cells and the target, as has been shown for anti-LFA-1 in other systems.[32] It is not clear whether adherence between these two cell types is a simple event requiring only one receptor ligand interaction or a complex event involving more than one interaction. For example, initial recognition and formation of the pockets may involve different receptors. Dissolution of the pockets may also be a receptor-mediated event. It is unlikely that anti-LFA-1 inhibits initial recognition, because directed discharge presumably occurred against a target cell. However, anti-LFA-1 may inhibit the formation of zones of apposition of NK cell and target membrane (Figure 5) that appear to seal the pockets. Alternatively, this antibody may promote the dissociation of NK cell target conjugates before granule constituents are fully solubilized.

References

1. Trinchieri G, Perussia B: Human natural killer cells: Biologic and pathologic aspects. Lab Invest 1984, 50:489–513
2. Dennert G: Mechanism of cell-mediated cytolysis by natural killer cells. Surv Synth Pathol Res 1985, 4:69–83
3. Henkart PA: Mechanism of lymphocyte-mediated cytotoxicity. Ann Rev Immunol 1985, 3:31–58
4. Zagury D: Direct analysis of individual killer T cells: Susceptibility of target cells to lysis and secretion of hydrolytic enzymes by CTL. Adv Exp Med Biol 1981, 146:149–163
5. Dennert G, Podack ER: Cytolysis by H-2 specific T killer cells. J Exp Med 1983, 157:1483–1495
6. Podack ER, Dennert G: Assembly of two types of tubules with putative cytolytic functions by cloned natural killer cells. Nature 1983, 302:442–445
7. Henkart MP, Henkart PA: Lymphocyte mediated cytolysis as a secretory phenomenon. Adv Exp Med Biol 1981, 146:227–242
8. Masson D, Tschopp J: Isolation of a lytic, pore-forming protein (perforin) from cytolytic T-lymphocytes. J Biol Chem 1985, 260:9069–9072
9. Podack ER, Young JD-E, Cohn ZA: Isolation and biochemical and functional characterization of perforin I from cytolytic T-cell granules. Proc Natl Acad Sci USA 1985, 82:8629–8633
10. Zalman LS, Brothers MA, Chin FJ, Muller-Eberhard HJ: Mechanism of cytotoxicity of human large granular lymphocytes: Relationship of the cytotoxic lymphocyte protein to the ninth component (C9) of human complement. Proc Natl Acad Sci USA 1986, 83:5262–5266
11. MacDermott RP, Schmidt RE, Caulfield JP, Hein A, Bartley GT, Ritz J, Schlossman SF, Austen KF, Stevens RL: Proteoglycans in cell-mediated cytotoxicity: Identification, localization, and exocytosis of a chondroitin sulfate proteoglycan from human cloned natural killer cells during target cell lysis. J Exp Med 1985, 162:1771–1787
12. Siliciano RF, Pratt JC, Schmidt RE, Ritz J, Reinherz EL: Activation of cytolytic T lymphocyte and natural killer cell function through the T11 sheep erythrocyte binding protein. Nature 1985, 317:428–430
13. Hercend T, Meuer S, Reinherz EL, Schlossman SF, Ritz J: Generation of a cloned NK cell line derived from the "null cell" fraction of human peripheral blood. J Immunol 1982, 129:1299–1305
14. Reinherz EL, Schlossman SF: The differentiation and function of human T lymphocytes: A review. Cell 1980, 19:821–827
15. Schmidt RE, Bartley G, Schlossman SF, Ritz J: Functional characterization of LFA-1 antigens in the interaction of human NK clones and target cells. J Immunol 1985, 135:1020–1025
16. Karnovsky MJ: A formaldehyde-glutaraldehyde fixative of high osmolality for use in electron microscopy (Abstr). J Cell Biol 1965, 27:137a
17. Payne CM, Glasser L, Fiederlein R, Lindberg R: New ultrastructural observations: Parallel tubular arrays in human T lymphoid cells. J Immunol Methods 1983, 65:307–317
18. Neighbour PA, Huberman HS, Kress Y: Human large granular lymphocytes and natural killing: ultrastructural studies of strontium-induced degranulation. Eur J Immunol 1982, 12:588–595
19. Grossi CE, Webb SR, Zicca A, Lydyard PM, Moretta L, Mingari MC, Cooper MD: Morphological and histochemical analyses of two human T-cell subpopulations

bearing receptors for IgM or IgG. J Exp Med 1978, 147:1405–1417
20. Grossi CE, Cadoni A, Zicca A, Leprini A, Ferrarini M: Large granular lymphocytes in human peripheral blood: Ultrastructural and cytochemical characterization of the granules. Blood 1982, 59:277–283
21. Smit JW, Blom NR, van Luyn M, Halie MR: Lymphocytes with parallel tubular structures: morphologically a distinctive subpopulation. Blut 1983, 46:311–320
22. Millard PJ, Henkart MP, Reynolds CW, Henkart PA: Purification and properties of cytoplasmic granules from cytotoxic rat LGL tumors. J Immunol 1984, 132:3197–3204
23. Ward JM, Reynolds CW: Large granular lymphocytic leukemia in F344 rats. Am J Pathol 1983, 111:1–10
24. Gruner SM, Cullis PR, Hope MJ, Tilcock CPS: Lipid polymorphism: The molecular basis of nonbilayer phases. Ann Rev Biophys Biophys Chem 1985, 14:211–238
25. Luzzati V, Husson F: The structure of the liquid-crystalline phases of lipid-water systems. J Cell Biol 1962, 12:207–219
26. Junger E, Reinauer H: Liquid crystalline phases of hydrated phosphatidylethanolamine. Biochim Biophys Acta 1969, 183:304–308
27. Stoeckenius W: Some electron microscopical observations on liquid-crystalline phases in lipid-water systems. J Cell Biol 1962, 12:221–229
28. Lucy JA, Glauert AM: Structure and assembly of macromolecular liquid complexes composed of globular micelles. J Mol Biol 1964, 8:727–748
29. Deamer DW, Leonard A, Tardieu A, Branton D: Lamellar and hexagonal lipid phases visualized by freeze-etching. Biochim Biophys Acta 1970, 219:47–60
30. Caulfield JP, Lewis RA, Hein A, Austen KF: Secretion in dissociated human pulmonary mast cells: Evidence for solubilization of granule contents before discharge. J Cell Biol 1980, 85:299–312
31. Bloom GD, Chakravaty N: Time course of anaphylactic histamine release and morphological changes in rat peritoneal mast cells. Acta Physiol Scand 1970, 78:410–418
32. Springer TA, Davignon D, Ho M-K, Kurzinger K, Martz E, Sanchez-Madrid F: LFA-1 and Lyt-2,3, molecules associated with T lymphocyte-mediated killing; and Mac-1, an LFA-1 homologue associated with complement receptor function. Immunol Rev 1982, 68:171–195

Acknowledgments

The authors would like to thank Drs. Stephen Furlong, Daniel Goodenough, and Alan Kleinfield for advice and conversations during the course of this work, Dr. Richard L. Stevens for reading the manuscript, Gail Bartley for excellent technical assistance, and Joanne Miccile for her expert typing and secretarial assistance.